

Recoil Behavior of the $\text{Cu}^{65}(p,pn)\text{Cu}^{64}$ Reaction*

E. R. MERZ† AND A. A. CARETTO, JR.

Department of Chemistry, Carnegie Institute of Technology, Pittsburgh, Pennsylvania

(Received December 11, 1961; revised manuscript received February 5, 1962)

The recoil behavior of the $\text{Cu}^{65}(p,pn)\text{Cu}^{64}$ reaction has been measured at bombarding energies from 100 Mev to 400 Mev by performing radiochemical integral recoil experiments. The fraction of the total Cu^{64} produced, found in the forward, backward, and right angle directions, shows definite structure with increasing bombarding energy. The data can be qualitatively interpreted by assuming the two-step cascade-evaporation mechanism to be relatively more important at low incident energies and a knock-on mechanism to be relatively more important at the higher incident energies. By means of a postulated velocity vector diagram, the average recoil range as a function of incident energy was calculated, and this calculated range was then converted to Cu^{64} kinetic energy by an experimentally determined range-energy relationship. The Cu^{64} was found to have an average kinetic energy of 380 kev at 105 Mev incident energy, to decrease to 105 kev at about 200 Mev, and then to increase to 195 kev at 400 Mev. This behavior is interpreted in terms of the cascade-evaporation mechanism and the knock-on mechanism.

INTRODUCTION

CONSIDERABLE interest has developed in the past few years in the study of excitation functions of the so called "simple" high energy nuclear reactions.¹ The $(p, 2 \text{ nucleon})$ reactions, which include (p,pn) , $(p,2p)$ and $(p,2n)$, have been studied by a number of workers and discussions of possible mechanisms have appeared in several reports.^{2,3}

Apparently, the two most important mechanisms described can be referred to as the one-step and two-step mechanisms. In the one-step mechanism, also known as the knock-on mechanism, the interaction of the incident particle is assumed to take place with only one nucleon and that both collision partners escape without further interaction. The residual excitation energy must be less than about 10 Mev so that no nucleon evaporation can ensue. In the two-step mechanism, the initial interaction is a small-angle (p,p') scattering in which only 10–20 Mev of excitation energy is deposited. According to this mechanism the nucleus then de-excites by particle evaporation.

The general features of the results of $(p, 2 \text{ nucleon})$ studies are: (1) A general energy independence of the excitation functions between 100 and 500 Mev; (2) An irregular dependence of (p,pn) cross section on target mass number (for example, the cross section for Fe^{54} and Ni^{58} differ by about 40% at 400 Mev.⁴ Several other cases of such effects have been found⁵); (3) The cross sections reported for (p,pn) reactions are generally larger than $(p,2p)$, and these in turn are larger than $(p,2n)$ by as much as an order of magnitude^{3,5}; (4) Studies of the ratio of $\sigma_{p,pn}$ to $\sigma_{p,2p}$ on several target

nuclei give results consistent with the interpretation of these reactions as proceeding mainly via the knock-on mechanism.^{3,6,7}

However, the study of excitation functions and cross section determinations does not provide sufficient information to decide unambiguously between the postulated reaction mechanisms. With this in mind, it was decided that a study of the recoil behavior of the product nuclei from $(p, 2 \text{ nucleon})$ reactions may provide insight to the mechanism. In this paper we report the results of an investigation of the $\text{Cu}^{65}(p,pn)\text{Cu}^{64}$ reaction, and in a subsequent paper the recoil behavior of the $\text{Zn}^{68}(p,2p)\text{Cu}^{67}$ reaction will be presented.

EXPERIMENTAL PROCEDURE

Integral recoil experiments, similar to those originally devised by Sugarman *et al.*,⁸ were performed by irradiating stacked foil targets in the internal beam of the Carnegie Institute of Technology synchrocyclotron. A schematic of the targeting arrangement is shown in Fig. 1. All targets consisted of 2-mil copper foils sandwiched between three 1-mil aluminum foils placed up-stream and down-stream from the copper. The purpose of the aluminum foils immediately adjacent to the copper target is to catch the Cu^{64} recoil atoms. Since it was expected that the range of recoil atoms in aluminum from a (p,pn) reaction would be of the order of 100 $\mu\text{g}/\text{cm}^2$ or less, the 1-mil aluminum foil ($\sim 7 \text{ mg}/\text{cm}^2$) was sufficiently thick to stop all recoils. The middle aluminum foils were used to monitor the proton beam by means of the reaction $\text{Al}^{27}(p,3p)\text{Na}^{24}$, the cross section of which has been determined.⁹ The end aluminum foils were used to determine the Cu^{64} blank. That is, the expected level of Cu^{64} produced in an aluminum foil of the same size and thickness as the catcher from impurities found in the aluminum. The

* Research performed under contract with the U. S. Atomic Energy Commission.

† Present address: Institut für Radiochemie, Kernforschungsanlage Jülich, Nordrhein-Westfalen, Germany.

¹ J. M. Miller and J. Hudis, *Ann. Rev. Nuclear Sci.* **9**, 159 (1959).

² H. P. Yule and A. Turkevich, *Phys. Rev.* **118**, 1591 (1960).

³ P. P. Strohal and A. A. Caretto, Jr., *Phys. Rev.* **121**, 1815 (1961).

⁴ S. Markowitz, F. S. Rowland, and G. Friedlander, *Phys. Rev.* **112**, 1295 (1958).

⁵ L. Remsberg (private communication).

⁶ A. A. Caretto and G. Friedlander, *Phys. Rev.* **110**, 1169 (1958).

⁷ W. R. Ware and E. O. Wiig, *Phys. Rev.* **122**, 1837 (1961).

⁸ N. Sugarman, M. Campos, and K. Wielgoz, *Phys. Rev.* **101**, 388 (1956).

⁹ H. G. Hicks, P. C. Stevenson, and W. E. Nervik, *Phys. Rev.* **102**, 1390 (1956).

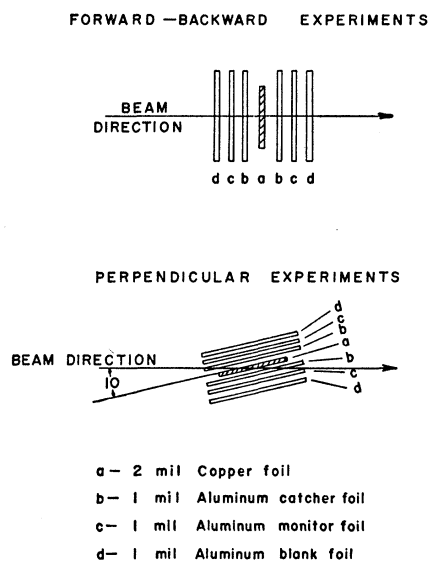


Fig. 1. Schematic diagram of targeting arrangement.

aluminum foils used were Alcoa, 99.99% pure, rolled to a uniform thickness of 1 mil. The copper target was standard 2-mil copper of 99.999% purity. In general, the aluminum blank foils showed a production of Cu^{64} from impurities of 1% or less of the amount of recoil Cu^{64} . This correction was negligible at all times but was included in the calculation of results. The aluminum foils used as catchers had a copper impurity of 1-3 ppm.

In each experiment copper activities were chemically isolated from all catchers and blank foils as well as the copper target foil. Standard chemical procedures were used which gave decontamination from other activities by factors of about 10^6 . Some runs were carried out in which the target foil was aligned at 80° to the beam (see Fig. 1). In all the experiments the quantity measured was the fraction of all the Cu^{64} product nuclei produced that recoiled either forward, backward, or at right angles to the incident beam. The fraction measured at right angles was the average of the activity found in the two catcher foils used in the 80° irradiations.

After chemically processing the target and catcher foils, the activity of the copper samples isolated was determined by use of a methane-flow end-window β -proportional counter. Each sample was counted with sufficient repetition and with proper statistics so that the 12.8-hr Cu^{64} activity could be determined with a precision of 3-4%.

To determine the fraction of the product recoils in any given direction it is only necessary to measure the ratio of activities. However, to compute the cross section for the reaction, it is necessary to make appropriate corrections to convert the observed activity to disintegration rates. Shelf geometries were determined by use of standardized National Bureau of Standards

sources, and later, by beta-gamma coincidence measurements on Na^{24} and Co^{60} . Air absorption correction factors, experimentally determined, as well as window absorption, back scattering, and self absorption and scattering correction factors were applied to convert the Cu^{64} activity to disintegration rates. In consideration of the decay scheme¹⁰ and under the actual conditions of measurement, it was assumed that 61% of all Cu^{64} transitions were detected. The target-monitor alignment and the experimental procedure for doing this have been discussed in a previous paper from this laboratory.³ The values chosen for the Na^{24} monitor excitation function were from the data of Hicks and Nervik.⁹

RESULTS

The excitation function of the $\text{Cu}^{65}(p,pn)\text{Cu}^{64}$ reaction is illustrated in Fig. 2. Also shown there, for comparison, are the experimental results of Yule and Turkevich² for the same reaction. The agreement can be considered excellent. The uncertainty in the points shown are indications of reproducibility from one run to the next. At energies of 100, 200, 300, and 400 Mev, five determinations were made at each energy. At 250 and 150 Mev two determinations were made, and, at the remaining lower energies, only one at each energy.

The fraction of the total Cu^{64} activity caught in the forward, backward, and perpendicular catcher foils from the recoil experiments is listed in Table I. Again, the results of the measurements made at the even hundreds of Mev are from 2-4 determinations each. The points at other energies are one or two determinations each. The average copper thickness used for all these runs was 45.4 mg/cm^2 . Illustrated in Fig. 3 are the recoil fractions as a function of bombarding energy.

The sources of errors in the $\text{Cu}^{65}(p,pn)\text{Cu}^{64}$ excitation function are in general not the same as those involved in the recoil fractions. The excitation function will be subject to uncertainties in the monitoring of the proton beam and possible misalignment of target foils. These errors should not be more than a few percent at any given energy. The uncertainty in the absolute value of the $\text{Al}^{27}(p,3n)\text{Na}^{24}$ cross section is about $\pm 10\%$. The uncertainties in counting efficiency and counting yield correction factors were estimated to be about $\pm 10\%$. Decay curve resolution, in this case, introduced an uncertainty of 2-3%. The chemical yield determinations were accurate to 1-2%. As a result of all these uncertainties the reported cross sections for the Cu^{64} excitation function are probably good to about $\pm 15\%$.

In measuring the fraction of the product recoil in any given direction, the uncertainties in beam monitoring, absolute value of the monitor cross section, and counting yields and efficiencies does not effect the results. In the recoil experiments, error may be intro-

¹⁰ D. Strominger, J. M. Hollander, and G. T. Seaborg, *Revs. Modern Phys.* **30**, 585 (1958).

TABLE I. Cross section and fraction of recoil activity.

Proton energy (Mev)	Cross section $\text{Cu}^{65}(p, pn)\text{Cu}^{64}$ (mb)	Fraction forward ($\times 10^5$)	Fraction backward ($\times 10^5$)	Fraction perpendicular ($\times 10^5$)
73	140.0	114.5	9.4	
85	116.0			61.0
105	104.0	87.5	45.1	
123	86.8	67.8	33.1	50.5
	87.1	74.3	40.1	63.7
	89.7			
	87.4			
	89.8			
168	66.9	52.8	18.6	51.3
	67.4			
210	62.9	51.7	16.5	43.2
	66.0	44.4	13.5	46.2
	61.0			
	66.2			
	64.5			
254	58.2	55.8	16.8	48.6
	56.3			
300	53.6	71.5	21.2	51.4
	52.9	68.2	21.2	45.4
	53.6			
	55.8			
	53.9			
400	51.3	90.5	26.3	78.9
	52.6	84.5	24.5	80.9
	52.1			
	46.8			
	46.7			

duced in misalignment of the catcher foils, weights and uniformity of catcher foils, decay curve analysis, chemical analysis, and those counting yield factors which are dependent on sample thickness. In these experiments these errors are not expected to result in uncertainties of the recoil fraction by more than $\pm 10\%$.

The product of the fraction of recoils forward times

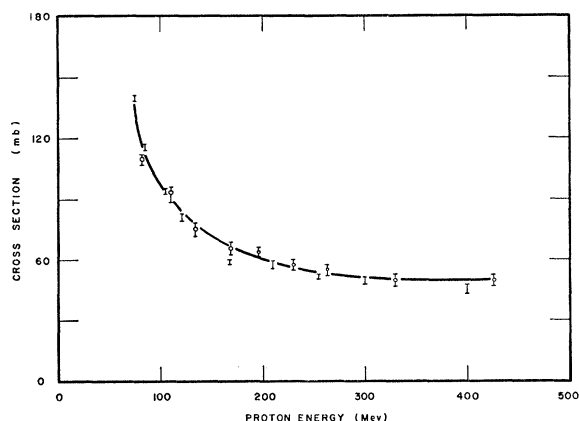


FIG. 2. Excitation function of the $\text{Cu}^{65}(p, pn)\text{Cu}^{64}$ reaction. Open circles=data of Yule and Turkevich, reference 2. Points without circles=this work.

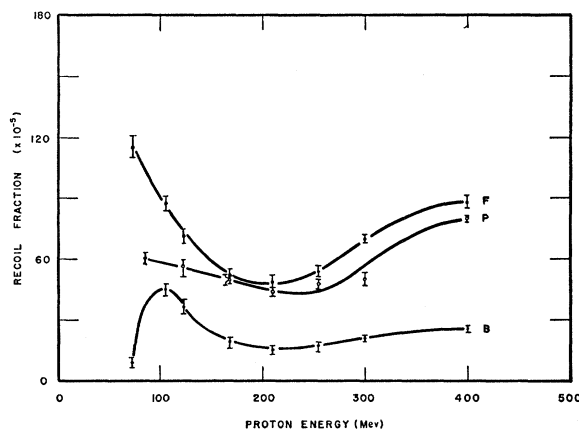


FIG. 3. Fraction of Cu^{64} recoil activity in the forward, backward, and perpendicular directions as a function of incident proton energy.

target thickness, FW , which is a quantity independent of target thickness for sufficiently thick targets, is in excellent agreement with similar quantities measured at 100 and 426 Mev by Yule and Turkevich.^{2,11} They report that at 426 Mev, FW , expressed in percent, is about 3.2% compared with this data at 400 Mev where the value is 3.9%. Similar agreement was realized at 110 Mev proton energy.

DISCUSSION

The objective of a study of the recoil behavior of nuclear reaction products is to determine the average momentum deposition in the reaction, the kinetic energies of the recoil fragments, and ultimately to be able to discern the reaction mechanisms. In integral recoil experiments, such as were performed here, the quantities measured were the recoil fractions forward, backward, and at right angles to the beam. No differential range measurements could be measured in these experiments. In order to estimate these quantities of interest a velocity vector diagram was assumed which was consistent with the possible reaction mechanisms. Any conclusions to be drawn from the recoil ranges, arrived at in this way, are obviously dependent on the particular vector diagram chosen. Therefore, it seems appropriate first to investigate, in terms of possible mechanisms, the qualitative features of the physical quantities measured, namely the recoil fractions.

Origin of Momentum Deposition in (p, pn) Reactions

If one assumes the knock-on mechanism there are two contributions to momentum deposition in (p, pn) reactions specifically and in $(p, 2 \text{ nucleon})$ reactions in general. If \mathbf{P}_i is the incident particle momentum and \mathbf{P}_1 and \mathbf{P}_2 the momenta of the two outgoing collision particles, then clearly the nuclear recoil momentum is

¹¹ Anthony Turkevich (private communication).

given by

$$\mathbf{P}_R = \mathbf{P}_i - \mathbf{P}_1 - \mathbf{P}_2.$$

Then assuming the validity of the impulse approximation, one can see that \mathbf{P}_R arises partially from a contribution of the interaction of the incident and collision particles with the nuclear potential and partially from a momentum resolution of the struck nucleon just before collision. This second momentum contribution can be thought of as the momentum which is transferred to the nucleus by the creation of a nucleon hole in the Fermi sea of nucleons. One can then write, for the total momentum imparted to the nucleus:

$$\mathbf{P}_R = \mathbf{P}_{\text{potential interaction}} + \mathbf{P}_{\text{hole}}.$$

If the two-step mechanism is assumed, then the momentum deposition arises from three processes. The effect of the interaction of the incident and out-going particles with the nuclear potential is again operative, and in addition, momentum is transferred to the nucleus as a result of the (p, p') interaction and from the evaporation of a nucleon.

Using a velocity-dependent nuclear potential, the momentum deposition by small angle (p, p') scattering was calculated assuming 20 Mev was transferred to the nucleus as excitation energy. The velocity-dependent nuclear potential chosen was the same as that reported by Glassgold¹² as derived from optical model calculations. Using this basis for calculation, the forward momentum imparted to the nucleus at 60 Mev incident energy, from (p, p') events alone, is almost 2 times that at 100 Mev, 4.8 times larger than at 200 Mev and about 20 times larger than at 300 Mev. Since the momentum imparted by the evaporation of a nucleon would be expected to be approximately isotropic in the system of the moving target nucleus, one can compare the recoil fractions illustrated in Fig. 3 with these expectations of the two-step model. The recoils found in the forward direction decrease by almost a factor of two between 60 Mev and 100 Mev in agreement with the results of the estimate. The recoils in the perpendicular direction show a very slight decrease up to 200 Mev. However, one would not expect the nuclear potential interaction to produce an appreciable effect in the perpendicular recoils. The complex behavior of the recoil fraction in the backward direction is not as easy to estimate as in the forward case. The assumption of small angle scattering need not apply at the lower energies. The larger size of the incident particle wave packet at the lower energies is expected to result in multiple nucleon interactions which may produce irregular behavior in the backward direction. However, the one low experimental point in the backward recoil fraction curve at 73 Mev cannot be considered as clear evidence that there really is a maximum in this curve.

One would expect that the total number of events

¹² A. E. Glassgold, *Revs. Modern Phys.* **30**, 419 (1958).

taking place by the cascade-evaporation mechanism would decrease with increasing incident energy, as is seen in the first part of the excitation function. At higher incident energies the deposition energy from the cascade increases. Thus, the probability of evaporating only one nucleon will decrease. It might be predicted, therefore, that the recoil fraction curves should reflect the same general shape, in the energy region of the two-step mechanism, as does the excitation function. This is seen to be qualitatively correct with the exception of the low backward fraction point at 73 Mev. This interpretation leads one to assume that the (p, pn) reaction takes place primarily by the two-step (p, p') evaporation mechanism for the lower incident energies. The importance of the two-step mechanism apparently then decreases with increasing energy.

As the incident energy increases above 200 Mev, the forward recoil fraction gradually increases until at 400 Mev it is again almost a factor of two times the value at the minimum at 200 Mev. If the knock-on mechanism becomes increasingly important at higher energy then the rise in the forward fraction must be related to this mechanism. The Monte Carlo cascade calculations support the contention of increasing knock-on contribution.^{2,13} The interaction of the incident particle with the nuclear potential is not expected to produce as important an effect at the higher energies.

It has been suggested^{1,4,13-15} that $(p, 2 \text{ nucleon})$ reactions at high energy probably take place in a zone near the nuclear surface. Rough calculations^{16,17} give (p, pn) cross sections of the correct order of magnitude provided that a realistic mass distribution near the nuclear surface is assumed, and suggest further¹⁶ that the interactions tend to take place on the side of the nucleus opposite the point of entry of the incident particle. This zone of successful (p, pn) interactions extends to deeper lying layers as the incident energy increases due in part to the larger escape probabilities of the higher energy collision partners. The effective collision nucleon is thus at a higher potential in collisions near 400 Mev than it is in collisions near 200 Mev, as may be conveniently visualized if one replaces the square well nuclear potential with one of tapering sides, such as a trapezoidal well. The increase in the potential "sampled" by the average target nucleon with increasing incident energy gives rise to a corresponding increase in the average "hole" momentum transferred to the nucleus.¹⁸ This anticipated increase is qualitatively consistent with the shape of the recoil fraction curves above 200 Mev as shown in Fig. 3. Thus, it appears on this basis that the knock-on mechanism

¹³ N. Metropolis, R. Bivins, M. Storm, A. Turkevich, J. M. Miller, and G. Friedlander, *Phys. Rev.* **110**, 185 (1958).

¹⁴ H. Tyrén, P. Hillman, and T. A. J. Maris, *Nuclear Phys.* **7**, 1 (1958); **7**, 10 (1958).

¹⁵ T. A. J. Maris, *Nuclear Phys.* **9**, 577 (1958).

¹⁶ P. A. Benioff, *Phys. Rev.* **119**, 324 (1960).

¹⁷ J. R. Grover (unpublished work).

¹⁸ J. R. Grover (private communication).

becomes increasingly important at the higher energies in agreement with the conclusions (based on other observations) of Yule,² Strohal,³ and Caretto⁶ and from the Monte Carlo cascade calculations¹³ despite the use of a rectangular nuclear well in the latter.

Nuclear Recoil-Velocity Vector Diagram

The velocity vector diagram which will be applied to the recoil fractions measured experimentally, in order to convert them into recoil ranges, is the same as that originally derived by Sugarman⁸ and Porile¹⁹ to explain high-energy-induced fission. This particular diagram was chosen for the comparison of the experimental results of this study because: (1) it provides a reasonable description and first order approximation of the kinematic model of the possible reaction mechanisms; (2) it enables the calculation of recoil ranges, albeit directly dependent on the particular form of the velocity diagram chosen; and (3) it provides an interesting comparison of the results of this study to other radiochemical recoil studies^{8,19} in which the same or a very similar diagram was employed. In this diagram it is assumed that the incident particle imparts a velocity v to the struck nucleus at an angle to the incident beam. The component of this velocity on the beam axis is defined as $v_{||}$; the component at right angles to the beam axis is referred to as v_{\perp} , see Fig. 4(a). The velocity v defines a cone about the beam axis with vertex at the point of interaction. The second step in the nuclear interaction imparts a velocity V in the system of the moving target nucleus and at an angle θ to the parallel component of v . In this treatment the angular distribution of θ is assumed isotropic. The velocity of the recoiling nucleus is given by a resolution of the velocities v and V at an angle θ_L in the laboratory system, see Fig. 4(b). The projection of the resolved velocity in any given direction is then related to the recoil range. In this study the range R was assumed to be proportional to the square of the velocity V . This is in essential agreement with the experimentally measured range-energy relation, determined by Porile²⁰ for mass 65–67 ions. The value of the proportionality constant relating range in $\mu\text{g}\cdot\text{cm}^{-2}$ to recoil kinetic energies in kev from the Porile data is $(0.174 \pm 0.015) \mu\text{g}\cdot\text{cm}^{-2}\cdot\text{kev}^{-1}$ for ranges between 20 and 125 $\mu\text{g}\cdot\text{cm}^{-2}$. The derivation of necessary equations relating the range with the recoil fraction in any given direction, and for the case of range proportional to energy, was performed by both Sugarman²¹ and Winsberg.²²

For convenience the quantity $\eta_{||}$ is defined as the ratio $v_{||}/V$ and η_{\perp} as the ratio v_{\perp}/V . Thus, the computation involves using the three experimentally measured quantities F , B , and P and enables one to calculate R , $\eta_{||}$, and η_{\perp} .

¹⁹ N. T. Porile and N. Sugarman, Phys. Rev. **107**, 1410 (1957).

²⁰ N. T. Porile (private communication).

²¹ N. Sugarman (private communication).

²² L. Winsberg (private communication).

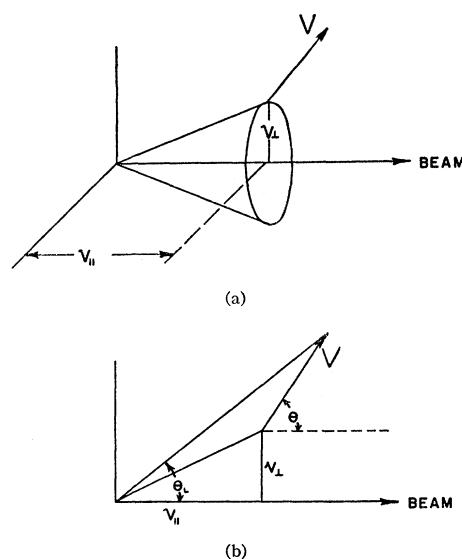


FIG. 4. Velocity vector diagrams illustrating the recoil model: (a) Three-dimensional; (b) Projection on beam axis.

It seems reasonable to assume that this vector diagram should be applicable to a study of the $(p, 2 \text{ nucleon})$ reaction recoil behavior. Both possible mechanisms, the one-step and the two-step, involve two separate interactions in which momentum is transferred to the target nucleus. However, it can be argued for both of the proposed mechanisms that no such simple resolution of velocity vectors is possible. In addition, the equations used to relate recoil fractions to recoil range are approximate in that terms with higher powers of η , particularly η_{\perp}^3 and $\eta_{||}^3$ have been neglected. For those cases where η_{\perp} is larger than 0.7 an error as large as 25% may be introduced. For these reasons the recoil range, arrived at by this method, should not be considered as an absolute range determination.

A graph of the Cu^{64} recoil ranges versus incident proton energy is shown in Fig. 5 and listed in $\mu\text{g}\cdot\text{cm}^{-2}$

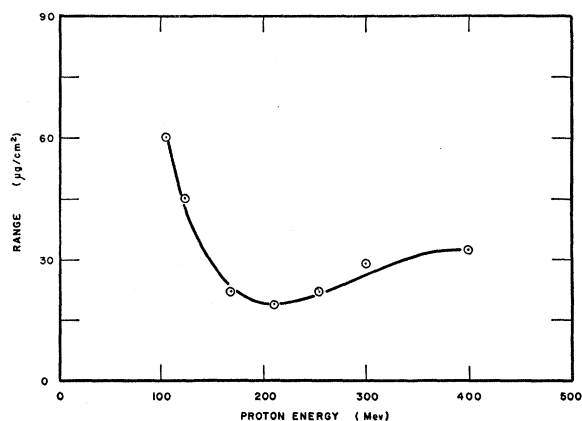


FIG. 5. Cu^{64} recoil range in copper (in $\mu\text{g}/\text{cm}^2$) as a function of incident proton energy.

TABLE II. Cu^{64} recoil ranges, kinetic energies, and η values.

Proton energy (Mev)	Cu^{64} recoil range ($\mu\text{g}/\text{cm}^2 \text{Cu}$)	$\eta_{11} = v_{11}/V$	$\eta_{12} = v_{12}/V$	Average Cu^{64} recoil kinetic energy (kev)
105	61.4	0.117		385
123	43.5	0.136	0.595	280
	46.1	0.126	0.495	
168	22.1	0.263	0.905	120
210	23.1	0.261	0.721	105
	14.3	0.372	0.912	
254	22.6	0.293	0.835	125
300	35.5	0.308	0.866	180
	29.1	0.350	0.906	
400	33.9	0.253	0.523	195
	34.8	0.231	0.457	

of copper in Table II together with the appropriate η values.

By use of the Porile range-energy relation it was possible to convert the ranges into Cu^{64} kinetic energies. The actual recoil kinetic energy associated with a given range was read off the Porile range-energy curve. This gives kinetic energies which may differ by as much as 10% from those determined by the previously mentioned range-energy proportionality constant. This is illustrated graphically in Fig. 6. As can be seen from the curve, there is apparently structure in the recoil kinetic energies as a function of bombarding energy. This is indeed surprising in view of the flat and smooth excitation function. The minimum in the curve at about 110 kev occurs at about 200-Mev incident proton energy. At higher proton energies the recoil kinetic energies increase to approximately 200 kev, and at a proton energy of 105 Mev the recoil kinetic energy is

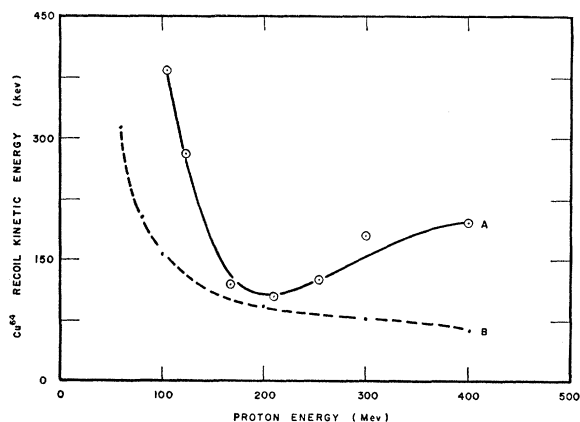


FIG. 6. Curve A: Cu^{64} recoil kinetic energies in copper (in kev) as a function of the incident proton energy. Curve B: Calculated Cu^{64} kinetic energy due to the interaction of the incident and collision nucleons with a velocity-dependent nuclear potential.

about 380 kev. Behavior of this type is strongly suggestive of a reaction in which more than one mechanism is operative.

The assumption that the velocity V is isotropic in the system of the moving target nucleus may not be valid. To remove this assumption requires making a new assumption as to the particular form of the anisotropy. Others¹⁹ have attempted to do this by assuming an $a + b \cos^2\theta$ angular distribution. The present authors do not feel that either the accuracy of the data or the reliability of the velocity vector diagram warrant a quantitative consideration of various anisotropic angular distributions. It can be concluded from these data, however, that a fairly large transversely peaked angular distribution is present.

Theoretical Estimates of Recoil Kinetic Energy from Knock-on Mechanism

It is of interest to make an estimate of the recoil kinetic energy by means of the knock-on mechanism. The discussion and approximate calculations which follow are in no way directly related to the previously described velocity vector recoil diagram. There is no obvious way of relating the quantities v and V to simple extreme calculations based on the kinematic models for momentum deposition. In fact, both the nuclear potential interaction and the hole momentum deposition contribute to both velocity vectors. However, it does seem useful to make estimates of the various sources of momentum deposition.

Momentum deposition from the hole left after collision takes place by the interaction of the incident particle with a nucleon of momentum $P_1 \leq P_f$. P_f is the maximum Fermi momentum and P_1 is the momentum of the collision nucleon before collision. Clements and Winsberg,²³ using a Monte Carlo calculation, computed the fraction of the number of incident particles on complex nuclei which are allowed by the Pauli exclusion principle. That is, they calculated the number of events in which both collision partners had a momentum greater than P_f after collision. In performing this calculation these authors chose a square well Fermi gas momentum distribution. Using their data, it was possible to calculate the average momentum, $\langle P_1 \rangle$, of the collision neutron for the $\text{Cu}^{65}(p, pn)\text{Cu}^{64}$ reaction before collision. This represents the momentum of the hole left behind, and hence the momentum deposition in the Cu^{64} nucleus which produces the recoil kinetic energy. Calculation of the average Cu^{64} recoil kinetic energy from the quantity $\langle P_1 \rangle$ leads to a value between 340–320 kev for protons between 70–440 Mev. This calculation was based on the assumption that all $(p, 2 \text{ nucleon})$ reactions are with nucleons at the top of the Fermi sea. A more realistic calculation, in which

²³ L. Winsberg and T. P. Clements, Phys. Rev. **122**, 1623 (1961).

interaction takes place with deeper lying nucleons, will lower the Cu^{64} recoil kinetic energy.

An estimate of the magnitude of the effect of the interaction of the nuclear potential with the incoming and outgoing particles was calculated using the results of the velocity dependent real part of the nuclear potential described by Glassgold¹² and used previously in this work in estimating the (p, p') effect. In this calculation the momentum transferred to the nucleus in a direction toward the incident particle was calculated using the low value of the nuclear potential at the high energies, i.e., about 3 Mev with 400-Mev incident protons. After collision takes place, an equal sharing of the incident energy by the two collision partners was assumed. The momentum transferred to the nucleus in the forward direction by the escape of both collision partners was then calculated using an effective nuclear potential of about 6 Mev at 200 Mev. The result of the calculation in terms of recoil kinetic energies is illustrated also in Fig. 6. It is interesting to note that the recoil kinetic energies, estimated by means of the knock-on mechanism do not reflect the shape of the recoil fraction curves as illustrated in Fig. 3.

Theoretical Estimates of Recoil Kinetic Energy from the Two-Step Mechanism

It is of interest to comment briefly on the recoil behavior expected from the two-step mechanism of cascade-evaporation. According to this mechanism one particle is emitted in direct cascade leaving behind excitation energy between about 10–20 Mev so that one nucleon can evaporate. It should be noticed that this mechanism has two reaction paths: (p, p'_n) and (p, n_p) where the first designation implies a proton-proton cascade followed by neutron evaporation. The second designation implies a proton-neutron cascade followed by proton evaporation. The interaction must produce a low-energy collision partner of about 10–15 Mev. This low-energy partner will in general be scattered at angles close to 90° to the incident beam. Hence, from the cascade interaction the recoil will occur close to right angles. This statement implies the assumption of isotropic internal nucleon momenta. Following the cascade interaction one nucleon is evaporated. This occurs almost isotropically in the center of mass system. Thus one might expect the fraction of the recoils occurring at right angles to be larger by this mechanism. The forward momentum deposition resulting from the interaction with the nuclear potential becomes negligible at the higher incident energies. Hence, the forward and perpendicular recoil fraction curves at the higher incident energies are not consistent with this mechanism.

An estimate of the magnitude of the recoil kinetic energy expected from the two-step mechanism can be made. The momentum transferred to the nucleus at

100 Mev resulting from the (p, p') interaction was calculated assuming 20 Mev was deposited as residual excitation energy. This momentum resulted in a recoil kinetic energy of 18 kev. If the assumption is made that the neutron evaporates with 10 Mev kinetic energy, allowing 10 Mev for binding energy, the resultant Cu^{64} momentum from both processes leads to a recoil kinetic energy of about 280 kev. Obviously the assumption that the neutron carries off all the excitation energy less binding energy will in general be incorrect. Thus, the two-step mechanism can account for fairly large recoil kinetic energies at low bombarding energies. Also, the kinetic energy should decrease with increasing incident energy due to the nature of nuclear potential interaction as was previously discussed. Therefore the two-step mechanism is in agreement with the shape of the recoil fraction curve (Fig. 3) for low incident energies.

Conclusions

It can be concluded that the integral recoil experiments described here have surprising structure in the recoil kinetic energy spectra. Furthermore, neither the one-step knock-on mechanism nor the two-step cascade evaporation mechanism can account for the magnitude of the recoil kinetic energies based on the simple treatments used in this study. The following statements summarize the conclusions which can be made:

- (1) The shape of the recoil fraction curves up to incident energies of 200 Mev are qualitatively consistent with the two-step mechanism in which the effect of the interaction of the incident particle with the nuclear potential is taken into account.
- (2) The increase in the recoil fraction curves at energies above 200 Mev can be qualitatively explained by the knock-on mechanism by assuming an increase in the hole momentum deposition with increasing incident energies.
- (3) Calculation of the average recoil kinetic energy arising from the hole momentum from the results of the Clements Monte Carlo calculation produces kinetic energies which are essentially independent of bombarding energy.
- (4) Calculation of the average recoil kinetic energy on the basis of the knock-on mechanism, by means of the potential interaction does not appear to have the correct shape when compared with the recoil fraction energy dependence.
- (5) Average recoil kinetic energies, calculated on the basis of the two-step mechanism, are consistent with the shape of the forward recoil fraction curve for incident energies below 150 Mev.

The over-all shape of the recoil fraction curves seems to be most consistent with the interpretation that the

two-step mechanism is relatively more important at low energies and the knock-on mechanism relatively more important at high energies.

There are three serious problems which must be further explored in order to increase our understanding of (p, pn) reactions specifically and $(p, 2 \text{ nucleon})$ reactions in general. The first of these relates to the irregular A dependence found for the cross section of (p, pn) reactions. It is clear that a better understanding of internal nucleon momenta would be an aid in explaining the A dependence and recoil behavior. A second serious problem is the uncertainty regarding the nature of the nuclear potential involved in the interaction of high-energy particles in complex nuclei. Experiments such as those performed here may provide some insight into the nature of the particle-potential interaction and as to whether a velocity-dependent potential is appropriate. Finally, until the differential

range and the total recoil angular dependence can be experimentally investigated, it will remain a matter of conjecture as to the proper recoil velocity vector diagram to use in integral experiments. The use of other possible recoil vector diagrams will be explored in a subsequent paper on the $\text{Zn}^{68}(p, 2p)\text{Cu}^{67}$ reaction.

ACKNOWLEDGMENTS

It is a pleasure to thank Dr. David L. Morrison and Dr. J. Robb Grover for many helpful discussions and advice. Also, the comments offered by Professor N. Sugarman and Dr. L. Winsberg are appreciated. We are indebted to Dr. N. T. Porile for making available the mass-67 range-energy data prior to publication. The authors wish to thank the operating staff of the Carnegie Institute of Technology proton synchrocyclotron for cooperation in carrying out the irradiations.